Catalysis Today 164 (2011) 489–494

Contents lists available at ScienceDirect

Catalysis Today

journal homepage: www.elsevier.com/locate/cattod

Direct NO decomposition over a Ce–Mn mixed oxide modified with alkali and alkaline earth species and CO_2-TPD behavior of the catalysts

Won-Jong Hong [a], Shinji Iwamoto [b], Masashi Inoue [a,*]

[a] Department of Energy and Hydrocarbon Chemistry, Graduate School of Engineering, Kyoto University, Katsura, Kyoto 615-8510, Japan
[b] Department of Chemistry and Chemical Biology, Graduate School of Engineering, Gunma University, Tenjin, Kiryu 376-8515, Japan

ARTICLE INFO

Article history:
Available online 15 December 2010

Keywords:
NO decomposition
Ce–Mn mixed oxide
Alkali
Alkaline earth
CO_2-TPD

ABSTRACT

A Ce–Mn mixed oxide with the Mn/(Ce + Mn) molar ratio of 0.25 (designated as CeMn) was prepared by the glycolthermal method, and NO decomposition activities of CeMn modified with various species (alkali and alkaline earth species and noble metals) were examined. Although CeMn itself exhibited only a low activity for the direct decomposition of NO into N_2 and O_2, CeMn modified with alkali or alkaline earth species exhibited significant activities. The CO_2-TPD experiment indicated that the NO decomposition activity of the catalysts was correlated with their basicities. The highest NO conversion was achieved by a Ba/CeMn system. The NO conversion on the Ba/CeMn catalyst increased with increasing reaction temperature, and 67% of NO conversion was attained at 800 °C. This catalyst retained a high activity (50% at 800 °C) even in the presence of 5% CO_2 in the feed gas.

1. Introduction

Nitrogen oxides (NO_x) formed by combustion cause severe detrimental environmental problems such as acid rain and photochemical smog. Catalytic NO_x reduction processes such as the three-way catalyst device for gasoline-fueled vehicles, NO_x storage-reduction (NSR) system for lean-burn engines, and selective catalytic reduction with ammonia (SCR) for large-scale combustion facilities have been developed so far. However, the amount of NO_x emission in urban area has significantly increased recently, and other effective deNO_x methods have been sought. Of various deNO_x strategies, direct decomposition of NO ($2NO \rightarrow O_2 + N_2$) is expected to be the most desirable because this process is quite simple and does not need any reductants such as NH_3, H_2, CO, or hydrocarbons.

Catalysts, such as precious metals [1,2], single metal oxides [3,4], Cu-ZSM-5 [5,6], Sr/La_2O_3 [7], Ba/MgO [8], alkali-doped Co_3O_4 [9–11], perovskites ($La_{1-x}Sr_xMO_3$ (M = Co, Fe, Mn) [12], $La_{1-x}Sr_xMn_{1-y}Ni_yO_3$ [13], $La_{1-x}Ba_xMn_{1-y}In_yO_3$ [14], $BaMnO_3$ [15], $SrFeO_3$ [16]) and C-type cubic rare earth oxides ($(Gd_{1-x-y}Y_xBa_y)_2O_{3-y}$ [17], $(Y_{1-x}Zr_x)_2O_{3+x}$ [18]) have been found to be effective for direct decomposition of NO. Recently, $Ba_{0.5}/BaY_2O_4$ mixed oxides were also reported to be active for this reaction [19]. Most of these catalysts contain alkali or alkaline earth elements, such as Na, K, Sr and Ba, in their oxide matrices [7–17,19]. However, the problem with these systems is the strong inhibition caused by the coexisting CO_2 because of its competitive adsorption with NO_x on the active sites of these catalysts [16,20]. Accordingly, it is necessary to develop catalysts having high NO decomposition activities even in the presence of CO_2.

We found that Ba–Ce–Co mixed oxides prepared by a polymerized complex method showed high NO decomposition activities [21]. The addition of other components to CeO_2 was also examined and it was found that Ce–Mn mixed oxides modified with Ba species showed improved activities [22].

In this study, we prepared a Ce–Mn mixed oxide by the glycothermal method and examined the NO decomposition activities of the Ce–Mn oxide modified with various species (alkali and alkaline earth species and noble metals). The catalysts were characterized by various techniques, and the correlation between NO decomposition activities of the catalysts and their behavior for the temperature-programmed desorption of CO_2 (CO_2-TPD) was investigated in detail.

2. Experimental

2.1. Preparation of the catalysts

A Ce–Mn mixed oxide sample with the Mn/(Ce + Mn) molar ratio of 0.25 (designated as CeMn) was prepared by the glycothermal method. Appropriate amounts of $Ce(CH_3COO)_3 \cdot 4H_2O$ and $Mn(CH_3COO)_2 \cdot H_2O$ were added to 100 ml of 1,4-butanediol, and this mixture was set in a 300-ml autoclave. After the autoclave was purged with nitrogen, the mixture was heated to 300 °C at a rate of 2.3 °C min^{-1} and kept at that temperature for 2 h. After

* Corresponding author. Tel.: +81 75 383 2478; fax: +81 75 383 2479.
E-mail address: inoue@scl.kyoto-u.ac.jp (M. Inoue).

0920-5861/$ – see front matter © 2010 Elsevier B.V. All rights reserved.
doi:10.1016/j.cattod.2010.10.063

the autoclave was cooled to room temperature, the resultant powder product was collected by centrifugation. It was washed with acetone, air-dried, and then calcined in air at 400 °C for 4 h.

Alkali, alkaline earth, and noble metal components were loaded on CeMn by an impregnation method using aqueous solutions of the corresponding metal nitrates, followed by calcination at 800 °C for 1 h (designated as M/CeMn, M denotes alkali, alkaline earth, or noble metal elements).

2.2. Direct NO decomposition

The catalytic tests for NO decomposition were carried out in a fixed-bed flow reactor made of quartz glass tubing with an inner diameter of 10 mm. The catalyst was pressed into a pellet, pulverized into 10–22 mesh size, and placed in the reactor. After the catalyst was heated at 800 °C in a He gas flow, the reaction gas containing 6000 ppm NO with He balance was introduced to the catalyst bed ($W/F = 1\ \mathrm{g\,s\,ml^{-1}}$, $\mathrm{SV} = 5000\ \mathrm{h^{-1}}$). The effluent gas was analyzed using a GL Science MicroGC 2002 gas chromatograph equipped with Molsieve 5A and Poraplot Q columns. The NO conversion was calculated on the basis of the formation of N_2:

$$\mathrm{NO\ \ conversion} = \frac{2[\mathrm{N_2}]_{\mathrm{out}}}{[\mathrm{NO}]_{\mathrm{in}}},$$

where $[N_2]_{out}$ is the N_2 concentration in the effluent gas and $[NO]_{in}$ is the NO concentration in the feed gas.

In the catalytic runs tested in the present study, only the by-product detected by Q-mass analysis (Pfeiffer Vacuum Omnistar GSD 301 O 1 Q-MASS spectrometer) was N_2O and selectivities for N_2 were >99%.

2.3. Characterization of the catalysts

Powder X-ray diffraction (XRD) patterns were recorded on a Shimadzu XD-D1 diffractometer using the Cu Kα radiation and a carbon-monochromator. Crystallite size of the catalysts was calculated from the half-height width of the diffraction peak using Scherrer's equation.

The specific surface area of the sample was calculated by the BET single-point method on the basis of nitrogen uptake measured at 77 K using a Shimadzu Micromeritics Flowsorb II 2300 sorptograph.

Temperature-programmed desorption profiles of CO_2 (CO_2-TPD) were obtained on a Bel Japan TPD-1-AT apparatus equipped with a quadrupole mass (Q-MASS) detector. Before the CO_2-TPD experiment, the samples (50 mg) were treated in situ in a 50 ml/min O_2 flow at 800 °C for 1 h, cooled to 50, 100, 200, or 500 °C in a 50 ml/min He flow, and, then, kept in a the same gas flow for 30 min. The samples were exposed to CO_2 (20 ml/min) at that temperature for 60 min, kept again in a 50 ml/min flow of He for 30 min, cooled to 50 °C, and then heated from 50 °C to 800 °C in the He gas flow at a rate of 10 °C/min^{-1} while monitoring CO_2 desorption.

Temperature-programmed desorption of NO (NO-TPD) was carried out in the fixed-bed flow reactor. The catalyst was heated at 550 °C for 30 min in He and cooled to 100 °C, and a gas composed of 6000 ppm NO and He balance was allowed to flow over the catalyst at $W/F = 1.0\ \mathrm{g\,s\,ml^{-1}}$ for 1 h. After the excess adsorptive gas was purged with an He flow, the catalyst was heated to 800 °C at a rate of 10 °C min^{-1} in the He flow, and the desorbed species were analyzed with a Pfeiffer Vacuum Omnistar GSD 301 O 1 Q-MASS spectrometer.

Table 1
BET surface areas and NO decomposition activities of M/CeMn catalysts (M = metal species added).

Catalyst	BET surface area (m^2/g)	NO conversion to N_2 (%)[a]		
		600 °C	700 °C	800 °C
CeMn[b]	22	2.5	4.0	6.3
5 wt.% Li	1	0.6	0.6	2.3
5 wt.% Na	6	0.7	5.3	12.5
5 wt.% K	10	4.3	16.0	34.6
5 wt.% Cs	15	4.6	12.9	22.0
5 wt.% Mg	15	1.5	2.7	4.6
5 wt.% Ca	15	4.2	13.5	26.2
5 wt.% Sr	29	14.6	35.2	49.9
5 wt.% Ba	28	23.3	57.3	67.7
5 wt.%V	2	–	–	0.2
5 wt.% Cr	10	–	–	–
5 wt.% Fe	24	–	0.3	0.4
5 wt.% Co	25	1.7	2.3	2.1
5 wt.% Ni	21	0.4	0.7	1.1
5 wt.% Cu	23	–	0.2	0.4
3 wt.% Rh	17	1.4	2.0	2.3
3 wt.% Pd	31	8.6	20.5	37.5
3 wt.%Ag	19	2.3	2.8	3.7
3 wt.% Pt	30	–	2.0	2.4
3 wt.% Pd/Al_2O_3[c]	105	17.4	48.5	65.5

[a] Catalyst, 0.50 g; 6000 ppm NO in He; $W/F = 1.0\ \mathrm{g\,s\,ml^{-1}}$.
[b] Ce–Mn mixed oxide with a Mn/(Ce + Mn) molar ratio of 0.25 calcined at 800 °C for 1 h.
[c] Al_2O_3 was purchased from Nanophase Technologies Corp.

3. Results and discussion

3.1. NO decomposition activity of CeMn modified with various components

Table 1 shows the NO decomposition activities of CeMn modified with alkali, alkaline earth, transition, and noble metal species. The Ce–Mn mixed oxide (CeMn) without additives exhibited quite a low activity. However, noticeable NO conversions were attained over CeMn modified with alkali, alkaline earth, and noble metal components except Li, Mg, Rh, Ag, and Pt. Among the catalysts examined, CeMn modified with K, Sr, Ba, and Pd exhibited high NO conversions. The Pd/CeMn catalyst was less active than Pd/Al_2O_3 catalyst; Al_2O_3 was purchased from Nanophase Technologies. The NO decomposition activity of CeMn decreased when transition metal species were loaded.

The BET surface area of CeMn calcined at 800 °C was 22 m^2/g. When it was modified with alkali, alkaline earth, and noble metal species, the surface area decreased except for loading of Sr, Ba, Pd, and Pt.

Fig. 1a and b shows the effects of the amounts of alkali and alkaline earth components on the activities of the M/CeMn catalysts. With the increase in the amount of K, Cs, Sr, and Ba, the activity significantly increased. High NO conversions were attained for 5 wt.% K/CeMn, 7 wt.% Cs/CeMn, 3 wt.% Sr/CeMn, and 3–10 wt.% Ba/CeMn, but further increase in the loading of these elements resulted in activity decrease, because of the decrease in the dispersion of alkali and alkaline earth species in the catalyst as discussed later.

3.2. Characterization of CeMn modified with alkali and alkaline earth components

Fig. 2 shows the XRD patterns of the CeMn and M/CeMn catalysts (M: alkali elements) calcined at 800 °C for 1 h. The XRD pattern of parent CeMn showed diffraction peaks at $2\theta = 28.3$, 33.1, 47.5, 56.5, 59.1, and 69.4, which were attributed to CeO_2 with a cubic fluorite structure (JCPDS #34-0394). No diffraction peaks due to Mn-related phases were recognized. This result is consistent with the report by Machida et al. [23]. They pre-

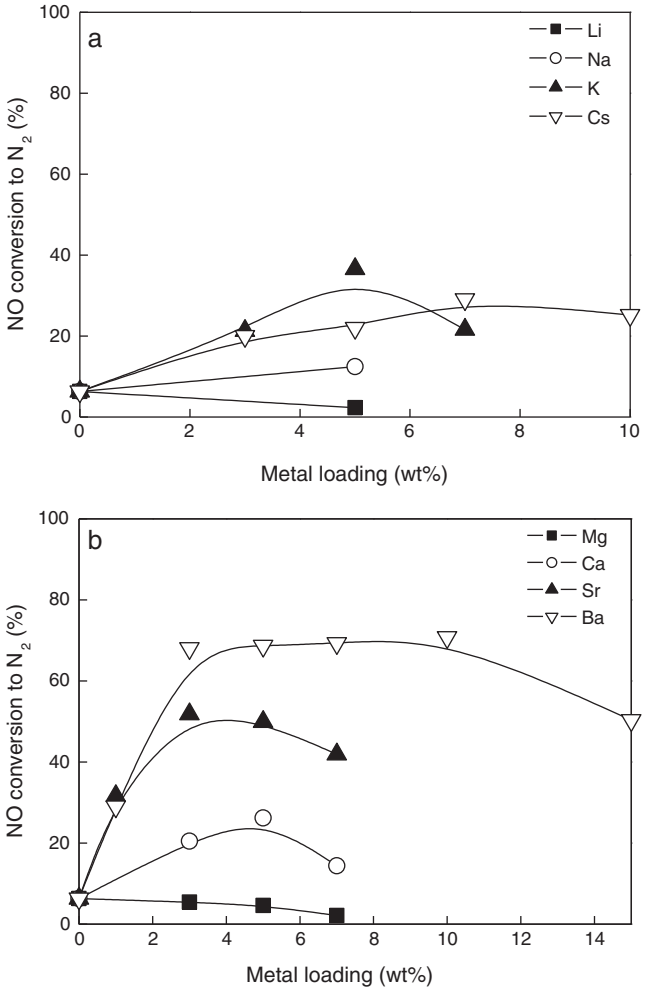

Fig. 1. Effect of the loading of alkali and alkaline earth components upon the NO decomposition activities of M/CeMn catalysts at 800 °C. (a) Alkali components, (b) alkaline earth components. *Reaction conditions*: catalyst, 0.50 g; 6000 ppm NO in He; $W/F = 1.0\ g\ s\ ml^{-1}$.

pared MnO_x–CeO_2 by a co-precipitation method, and found that Mn_2O_3 was crystallized in the samples with Mn/(Mn + Ce) > 0.75, whereas the samples with Mn/(Mn + Ce) < 0.5 showed broad peaks attributable to CeO_2. For the CeMn samples containing alkali components, peaks due to both CeO_2 and alkali manganites, $Li_4Mn_5O_{12}$ (JCPDS #46-0810) (Fig. 2(a)) [24,25], $Na_xMnO_2{\cdot}H_2O$ (Fig. 2(b)) [26–29], and $K_xMnO_2{\cdot}H_2O$ (Fig. 2(c)) [26–29], and $Cs_xMnO_2{\cdot}H_2O$ (Fig. 2(d)) [30,31], were detected. In addition, incorporation of alkaline species caused sharpening of the peaks due to CeO_2, indicating that the alkali components facilitated the growth of CeO_2 crystals.

Fig. 3 shows the XRD patterns of M/CeMn catalysts (M: alkaline earth elements). Only diffraction peaks due to CeO_2 are observed, and no diffraction peaks due to the phases containing Mn and/or alkaline earth elements are recognized. This result indicates the high dispersion of alkaline earth ions on these catalysts.

In order to see the basicity of the catalyst, CO_2-TPD experiment was carried out, and the results are shown in Figs. 4 and 5. The CO_2-TPD profile for CeMn alone showed a peak at ~100 °C (Fig. 4e). The peak observed at ~700 °C for Li/CeMn and Na/CeMn is due to the decomposition of alkali carbonates; this deduction was arrived at on the basis of the thermal analyses of the corresponding metal carbonates carried out under the same conditions as the present CO_2-TPD experiment (data not shown). Addition of alkaline earth species on CeMn caused the increase in the intensity of the desorption peak at ~100 °C and expansion of the tail toward high

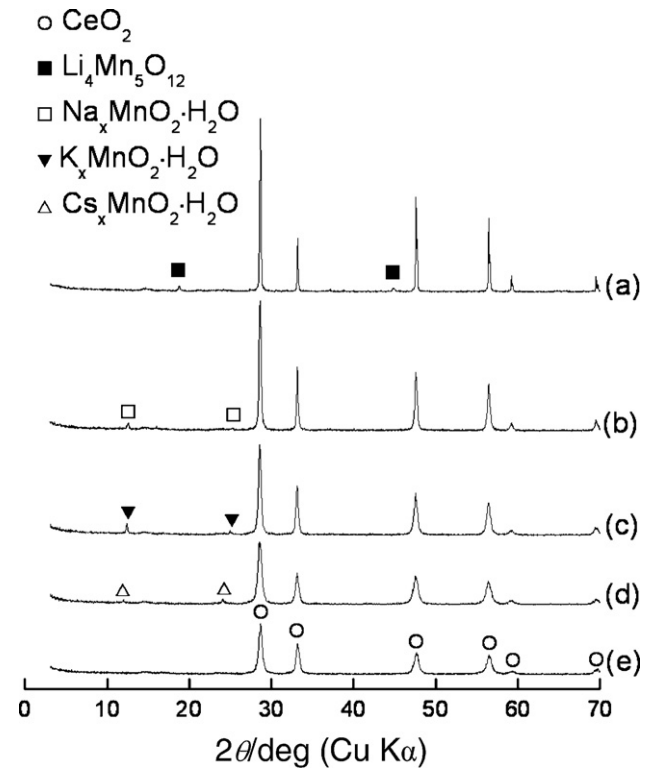

Fig. 2. XRD patterns of M/CeMn catalysts (M: alkali elements). (a) Li, (b) Na, (c) K, (d) Cs, and (e) CeMn alone.

temperatures, indicating that the addition of alkaline earth components increased the number of basic sites together with their basicities. In addition, a large desorption peak appeared at ~480 °C for Ca/CeMn due to the decomposition of $CaCO_3$, which was also confirmed by a separate experiment.

Fig. 6 shows the correlation between NO conversion and CO_2 uptake (based on the desorption of CO_2 in TPD experiment) by the

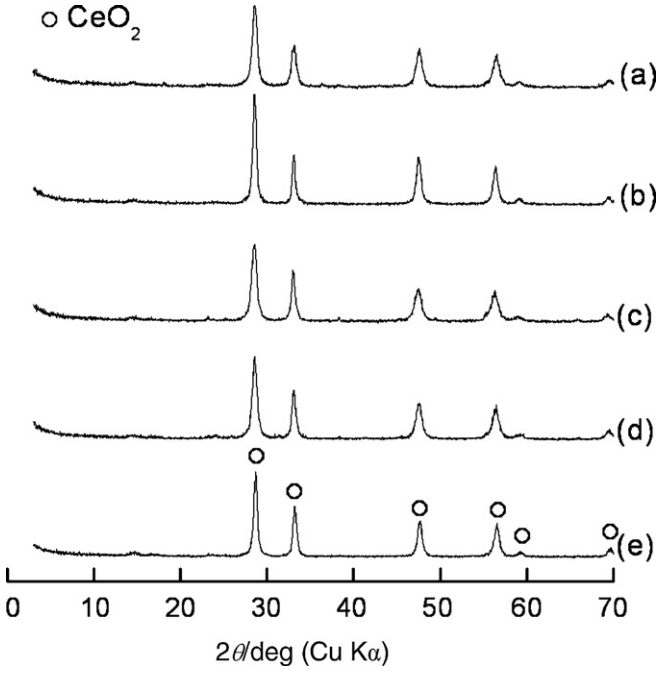

Fig. 3. XRD patterns of M/CeMn catalysts (M: alkaline earth elements). (a) Mg, (b) Ca, (c) Sr, (d) Ba, and (e) CeMn alone.

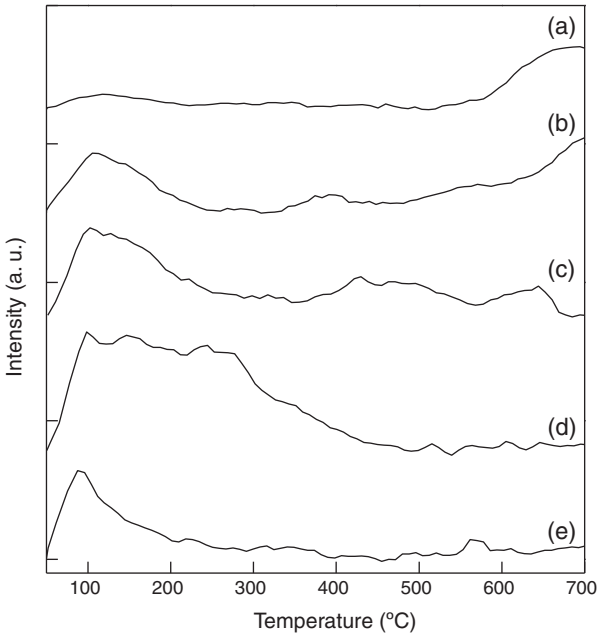

Fig. 4. CO_2-TPD profiles of M/CeMn catalysts (M: alkali elements): CO_2 was adsorbed at 50 °C for 1 h. (a) Li, (b) Na, (c) K, (d) Cs, and (e) CeMn alone.

catalyst, the CO_2 uptake having been determined by subtracting the CO_2 formation due to the decomposition of metal carbonate. Although CeMn showed only a small CO_2 uptake, loading of alkali and alkaline earth species apparently increased CO_2 uptake except for Li; the maximum CO_2 uptake was attained by the Ba-loaded sample. NO conversion also increased by the addition of these species, indicating that the NO decomposition activities of the catalysts are correlated with their basic properties and numbers of basic sites.

The effect of the amount of Ba on the basic properties of the Ba/CeMn catalysts was investigated by the CO_2-TPD technique. Since the addition of Ba to CeMn increased the intensity of the peak at ~100 °C (Fig. 5d), the integral intensity of the ~100 °C peak corresponding to CO_2 uptake was plotted against Ba loading (Fig. 7). Large CO_2 uptakes were observed for the samples with Ba loadings of 3–10 wt.%, and further increase in Ba loading gradually decreased CO_2 uptake, which seems to be due to decreased dispersion of the Ba species in the catalysts. This argument is supported by the XRD patterns of the 10 and 15 wt.% Ba/CeMn catalysts; peaks due to $BaMnO_{3-\delta}$, and $BaCO_3$, were detected besides the peaks due to CeO_2 (data not shown). In Fig. 7, the NO decomposition activities are also plotted. Both the CO_2-uptake and the NO-conversion plots had an essentially identical shape, indicating again that the NO decomposition activity of the catalyst is correlated with its basic property.

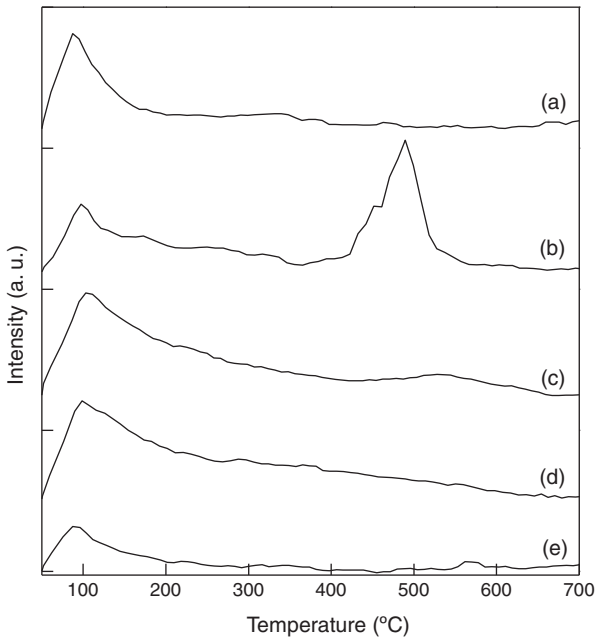

Fig. 5. CO_2-TPD profiles of M/CeMn catalysts (M: alkaline earth elements): CO_2 was adsorbed at 50 °C for 1 h. (a) Mg, (b) Ca, (c) Sr, (d) Ba, and (e) CeMn alone.

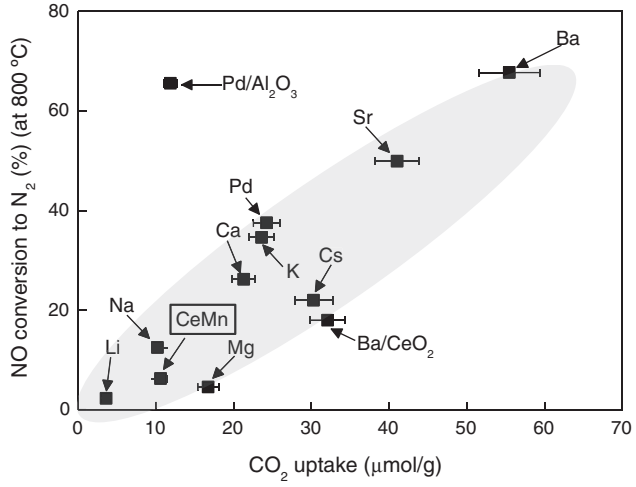

Fig. 6. Correlation between NO conversion and CO_2 uptake over Ce–Mn mixed oxide modified with various metal species (alkali and alkaline earth species and noble metals).

Fig. 8 shows CO_2-TPD profiles of the 5 wt.% Ba/CeMn catalyst after CO_2 was adsorbed at various temperatures. The CO_2 desorption peaks shifted to higher temperatures and the intensity decreased with increasing the CO_2 adsorption temperature. It must be noted that CO desorption peak was not significant; the desorption of CO should be observed when CO_2 is dissociatively adsorbed on the catalyst. Moreover, the FT-IR spectra of the catalyst after CO_2 adsorption showed the peaks due to carbonate species, and essentially identical spectra were obtained when CO_2 was adsorbed at higher temperatures, indicating that the nature of the basic sites did not change at high temperatures.

Fig. 9 shows NO-TPD profiles of CeMn and 5 wt.% Ba/CeMn catalysts. In this figure, desorption curves of N_2 and O_2 formed from NO molecules adsorbed are also shown. For parent CeMn, NO desorp-

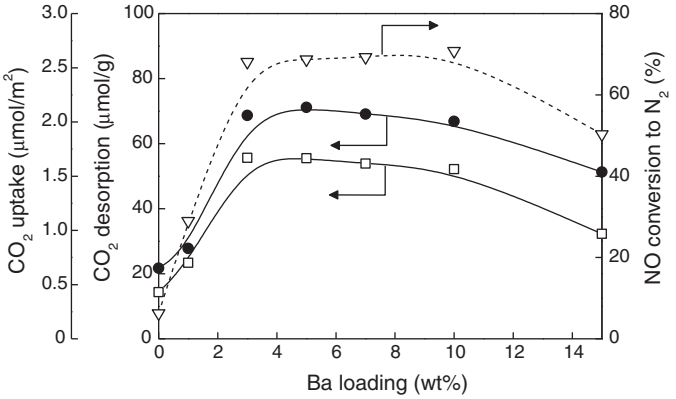

Fig. 7. Effect of the Ba-loading upon the CO_2 uptake (□, based on catalyst weight; ●, based on catalyst surface area) and upon NO conversion (▽) on the Ba/CeMn catalyst.

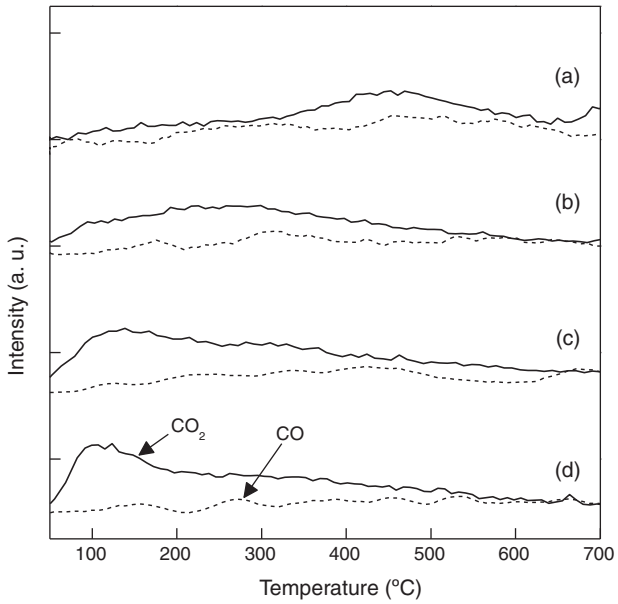

Fig. 8. CO_2-TPD profiles of the 5 wt.% Ba/CeMn catalyst after CO_2 was adsorbed at: (a), 500 °C; (b), 200 °C; (c), 100 °C; and (d), 50 °C.

tion took place at two different temperature ranges; one at ~250 °C and the other at ~480 °C. In the latter temperature range, NO desorption was associated with the desorption of O_2, indicating that surface nitrate species decomposed in this temperature range. A small O_2 desorption peak was also observed at ~750 °C. However, N_2 desorption peak was not observed over the entire temperature range, suggesting that all the nitrogen oxide species were consumed before the catalyst exhibited the NO decomposition activity. On the other hand, for the Ba/CeMn catalyst, significant N_2 formation albeit with low intensity was observed in the high temperature range, and the NO desorption peak associated with the O_2 desorption shifted to higher temperature region (~550 °C), indicating that the addition of Ba to CeMn produced considerably strong NO adsorption sites on the surface. Therefore, one possible explanation for the NO decomposition is that NO species adsorbed on the Ba sites migrate to CeMn, where NO is decomposed by the redox property of the Mn or Ce ions.

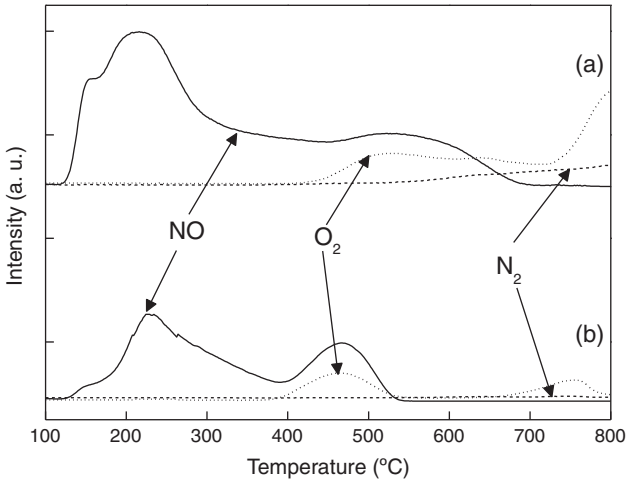

Fig. 9. NO-TPD profiles of: (a), 5 wt.% Ba/CeMn; and (b), CeMn alone.

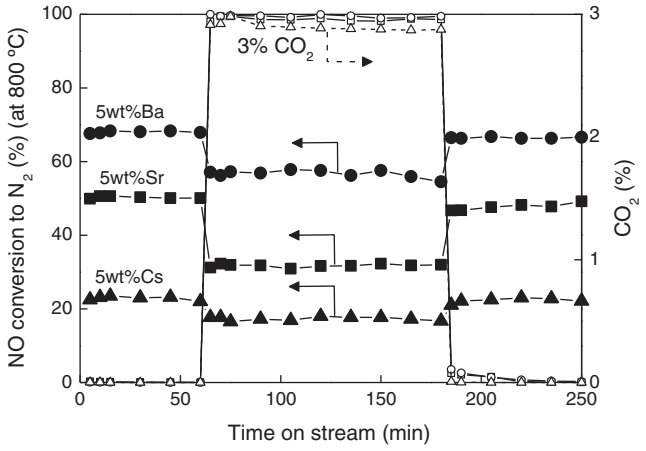

Fig. 10. Effect of CO_2 on NO conversion to N_2 (closed symbols) over 5 wt.% Ba/CeMn (circle), 5 wt.% Sr/CeMn (square), and 5 wt.% Cs/CeMn (triangle) catalysts. *Reaction conditions*: catalyst, 0.50 g; 3000 ppm NO in He; $W/F = 1.0\,g\,s\,ml^{-1}$; temperature, 800 °C; The CO_2 contents in the effluent gas are shown by open symbols.

3.3. Influence of CO_2 on the NO decomposition activities of alkali and alkaline earth metal-loaded catalysts

CO_2 is one of the major components in exhaust gases and has negative effects for NO decomposition [32–34]. Tofan et al. [32] reported that NO decomposition over three perovskite catalysts, $La_{0.87}Sr_{0.13}Mn_{0.2}Ni_{0.8}O_{3-\delta}$, $La_{0.66}Sr_{0.34}Ni_{0.3}Co_{0.7}O_{3-\delta}$, and $La_{0.8}Sr_{0.2}Cu_{0.15}Fe_{0.85}O_{3-\delta}$, was reversibly inhibited by CO_2 at high temperatures (600–650 °C), due to the competitive adsorption of CO_2 and NO on the same surface oxygen sites. Liu et al. [33] also reported that CO_2 inhibition for $Ag/La_{0.6}Ce_{0.4}CoO_3$ catalyst was quite large (NO conversion decreased from 65% to 45%), although the inhibition was not permanent but reversible. Hence, we anticipated that co-feeding CO_2 would have a large negative effect on the activities of CeMn modified with alkali and alkaline earth components, because these catalysts have considerable numbers of basic sites. Fig. 10 shows the effect of CO_2 on the NO conversion to N_2 over Cs-, Sr-, and Ba-loaded CeMn catalysts. The reaction was carried out at 800 °C. During the course of the reaction, 3% of CO_2 was introduced, and after some reaction period, CO_2 feed was stopped. Although Cs-, Sr-, and Ba-loaded CeMn catalysts exhibited stable NO conversions (23%, 50%, and 67%, respectively) in the absence of CO_2 in the feed gas, they decreased to 17%, 31%, and 57% on an introduction of 3% of CO_2. However, the activities were promptly recovered after the CO_2 feed was stopped. Iwakuni et al. [34] carried out a similar experiment for $Ba_{0.8}La_{0.2}Mn_{0.8}Mg_{0.2}O_3$ catalyst prepared by a conventional solid-state method: they reported that N_2 yield decreased from 70% to 30% on addition of 1% of CO_2 to the feed gas at 850 °C, and that, after cutting the CO_2 feed, the original NO conversion was recovered gradually over a period of a few hours. They found that CO was desorbed from their catalyst at 700 °C in the CO_2-TPD experiment, almost no CO_2 desorption being detected. They concluded that adsorption of CO_2 on their catalyst is quite strong and dissociative, producing CO and adsorbed oxygen species on the surface. In the present work, however, the CO desorption was not detected in the CO_2-TPD profile for Ba/CeMn. Furthermore, the CO_2 desorption peak was observed at ~100 °C (Fig. 5), which is much lower than the desorption temperature of NO (~550 °C) (Fig. 9). This feature indicates that adsorption of CO_2 on the Ba/CeMn catalyst is quite weaker than that of NO. Therefore, the Ba/CeMn catalyst suffers from CO_2 inhibition to a much lesser extent.

Fig. 11 shows NO conversion as a function of CO_2 concentration over the 5 wt.% Ba/CeMn catalyst. The NO conversion monotonically

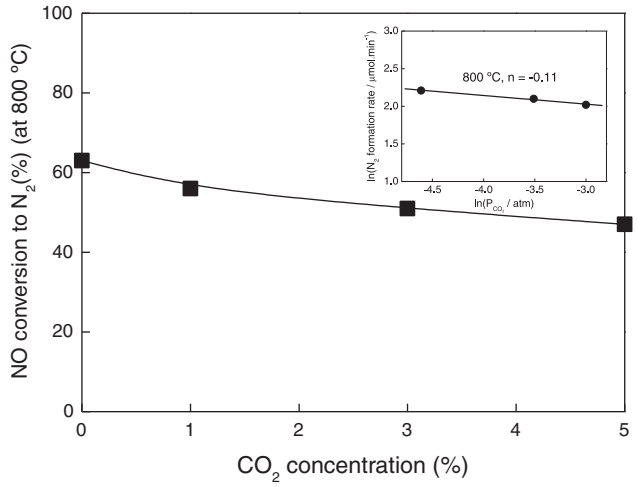

Fig. 11. NO conversion as a function of CO_2 concentration over 5 wt.% Ba/CeMn catalyst at 800 °C. The inset: N_2 formation rate as a function of CO_2 partial pressure at 800 °C. *Reaction conditions*: catalyst, 0.50 g; 3000 ppm NO in He in the presence of various concentrations of CO_2; $W/F = 1.0\ g\ s\ ml^{-1}$.

decreased with increasing CO_2 concentration. However, even in the presence of 5% CO_2 in the feed gas, the catalyst preserved a relatively high activity. The reaction order with respect to CO_2 partial pressure at 800 °C was −0.11 (Fig. 11, the inset). In a previous work, we found that the reaction order with respect to O_2 was −0.25 [22]. The decrease in the activity of 5 wt.% Ba/CeMn catalyst by the presence of O_2 in the feed was more significant as compared with the P_{CO_2} dependence of the activity shown in this paper. Furthermore, comparison of this value with that of the $Ba_{0.8}La_{0.2}Mn_{0.8}Mg_{0.2}O_3$ catalyst (−0.32) [34] suggests the high potential of the present Ba/Ce–Mn catalyst for practical deNO_x application.

4. Conclusions

Direct decomposition of NO over a Ce–Mn mixed oxide modified with various metal species (alkali and alkaline earth species and noble metals) was examined, and it was found that the Ce–Mn mixed oxide modified with alkali and alkaline earth species exhibited high activities, although the parent Ce–Mn mixed oxide exhibited quite a low activity. The highest activity was observed for Ba/CeMn. The XRD analyses suggested high dispersion of alkaline earth ions on the Ce–Mn mixed oxides. The CO_2-TPD results indicated that the NO decomposition activities of the catalysts were correlated with their basic properties. A high NO conversion of 67% was attained over 5 wt.% Ba/Ce–Mn at 800 °C in the absence of CO_2 in the feed gas, and even in the presence of 5% of CO_2, 50% of NO conversion was retained, suggesting the high potential of the Ba/CeMn mixed oxide catalysts for practical application in NO_x emission control.

Acknowledgments

The authors thank Dr. Seiichiro Imamura and Dr. Hiroyoshi Kanai of Kyoto University for their invaluable advice.

References

[1] A. Amirnazm, J.E. Benson, M. Boudart, J. Catal. 30 (1973) 55–65.
[2] R.J. Wu, T.Y. Chou, C.T. Yeh, Appl. Catal. B: Environ. 6 (1995) 105–116.
[3] E.R.S. Winter, J. Catal. 22 (1971) 158–170.
[4] E.R.S. Winter, J. Catal. 34 (1974) 431–439.
[5] M. Iwamoto, H. Yahiro, Y. Mine, S. Kagawa, Chem. Lett. 18 (1989) 213–216.
[6] M. Iwamoto, H. Hamada, Catal. Today 10 (1991) 57–71.
[7] M.A. Vannice, A.B. Walters, X. Zhang, J. Catal. 159 (1996) 119–126.
[8] S.B. Xie, M.P. Rosynek, J.H. Lunsford, J. Catal. 188 (1999) 24–31.
[9] P.W. Park, J.K. Kil, H.H. Kung, M.C. Kung, Catal. Today 42 (1998) 51–60.
[10] M. Haneda, Y. Kintaichi, N. Bion, H. Hamada, Appl. Catal. B: Environ. 46 (2003) 473–482.
[11] M. Haneda, Y. Kintaichi, H. Hamada, Appl. Catal. B: Environ. 55 (2005) 169–175.
[12] Y. Teraoka, H. Fukuda, S. Kagawa, Chem. Lett. 19 (1990) 1–4.
[13] Y. Teraoka, T. Harada, S. Kagawa, J. Chem. Soc. Faraday Trans. 94 (1998) 1887–1891.
[14] T. Ishihara, M. Ando, K. Sada, K. Takiishi, K. Yamada, H. Nishiguchi, Y. Takita, J. Catal. 220 (2003) 104–114.
[15] H. Iwakuni, Y. Shinmyou, H. Yano, H. Matsumoto, T. Ishihara, Appl. Catal. B: Environ. 74 (2007) 299–306.
[16] H. Iwakuni, Y. Shinmyou, H. Matsumoto, T. Ishihara, Bull. Chem. Soc. Jpn. 80 (2007) 2039–2046.
[17] N. Imanaka, T. Masui, H. Masaki, Adv. Mater. 19 (2007) 3660–3663.
[18] H. Masaki, T. Masui, N. Imanaka, J. Alloys Compd. 451 (2008) 406–409.
[19] K. Goto, H. Matsumoto, T. Ishihara, Top. Catal. 52 (2009) 1776–1780.
[20] M. Machida, S. Ogata, K. Yasuoka, K. Eguchi, H. Arai, Stud. Surf. Sci. Catal. 75 (1993) 2645–2648.
[21] S. Iwamoto, T. Yasuda, M. Inoue, Adv. Technol. Mater. Mater. Proc. J. 4 (2002) 58–61.
[22] S. Iwamoto, R. Takahashi, M. Inoue, Appl. Catal. B: Environ. 70 (2007) 146–150.
[23] M. Machida, M. Uto, D. Kurogi, T. Kijima, Chem. Mater. 12 (2000) 3158–3164.
[24] Y. Tanaka, Q.W. Zhang, F. Saito, Powder Technol. 132 (2003) 74–80.
[25] Y. Tian, D.R. Chen, X.L. Jiao, Y.Z. Duan, Chem. Commun. (2007) 2072–2074.
[26] Q. Feng, H. Kanoh, Y. Miyai, K. Ooi, Chem. Mater. 7 (1995) 1226–1232.
[27] R.J. Chen, T. Chirayil, P. Zavalij, M.S. Whittingham, Solid State Ionics 86–88 (1996) 1–7.
[28] O. Prieto, M. Del Arco, V. Rives, J. Mater. Sci. 38 (2003) 2815–2824.
[29] S. Bach, J.P. Pereira-Ramos, P. Willmann, Electrochim. Acta 52 (2006) 504–510.
[30] S. Ching, S.M. Hughes, T.P. Gray, E.J. Welch, Micropor. Mesopor. Mater. 76 (2004) 41–49.
[31] C.L. Lopano, P.J. Heaney, J.E. Post, Am. Miner. 94 (2009) 816–826.
[32] C. Tofan, D. Klvana, J. Kirchnerova, Appl. Catal. B: Environ. 36 (2002) 311–323.
[33] Z.M. Liu, J.M. Hao, L.X. Fu, T.L. Zhu, Appl. Catal. B: Environ. 44 (2003) 355–370.
[34] H. Iwakuni, Y. Shinmyou, H. Yano, K. Goto, H. Matsumoto, T. Ishihara, Bull. Chem. Soc. Jpn. 81 (2008) 1175–1182.